Available online at www.sciencedirect.com
SCIENCE DIRECT
Journal of Organometallic Chemistry 691 (2006) 387–394
Journal of Organometallic Chemistry
www.elsevier.com/locate/jorganchem

Triosmium–antimony clusters containing the μ,η²-phenylene ligand: Unusually long osmium–osmium bonds

Guizhu Chen, Mingli Deng, Chee Keong Don Lee, Weng Kee Leong *, Jialin Tan, Chuen Tse Tay

Department of Chemistry, National University of Singapore, Kent Ridge, Singapore 119260, Singapore

Received 29 August 2005; received in revised form 7 September 2005; accepted 7 September 2005
Available online 14 October 2005

Abstract

The reaction of the osmium–antimony cluster $Os_3(\mu\text{-}H)(\mu\text{-}SbPh_2)(\mu_3,\eta^2\text{-}C_6H_4)(CO)_9$ with $AsPh_3$ at room temperature afforded the *o*-phenylene cluster $Os_3(\mu\text{-}H)(SbPh_2)(\mu_2,\eta^2\text{-}C_6H_4)(CO)_9(AsPh_3)$ by nucleophilic addition via a metal–metal bond cleavage, and the substitution product $Os_3(\mu\text{-}H)(SbPh_2)(\mu_3,\eta^2\text{-}C_6H_4)(CO)_8(AsPh_3)$. It reacted with ^{t}BuNC to afford the adduct $Os_3(\mu\text{-}H)(SbPh_2)(\mu_2,\eta^2\text{-}C_6H_4)(CO)_9(CN^tBu)$ quantitatively. This adduct isomerised slowly on standing via migration of the isonitrile, while photolysis led to decarbonylation to $Os_3(\mu\text{-}H)(SbPh_2)(\mu_2,\eta^2\text{-}C_6H_4)(CO)_8(CN^tBu)$. All the products have been characterised completely, including by X-ray crystallography, and their structures exhibit very long Os–Os bonds.

Keywords: Osmium; Antimony; Phenylene; Clusters; Arsine; Isonitrile

1. Introduction

Main group-transition metal cluster compounds continue to be of interest because of expectations that they would show structural and reactivity patterns that may be quite unlike those of the homometallic main group or transition metal clusters. Antimony-containing clusters are the least represented among the group 15 elements [1]. A few years ago, we embarked on a study to examine the chemistry of osmium–antimony clusters [2], and found much chemistry that is very unlike that of even the next lighter congener, arsenic [3]. One of the clusters that we have studied fairly extensively is $Os_3(\mu\text{-}H)(\mu\text{-}SbPh_2)(\mu_3,\eta^2\text{-}C_6H_4)(CO)_9$, **1**, which we first obtained as one of the products from the thermolysis of $Os_3(CO)_{11}(SbPh_3)$ [2e]. Among the interesting chemistry that we have uncovered were its abilities to catalyse the cyclotrimerisation of diphenylacetylene [2b], and to undergo nucleophilic addition via metal–metal bond cleavage [2a]. The products from the latter reactions exhibited the longest Os–Os bonds (>3.2 Å) reported, much longer than a proposed maximum of 3.05 Å [4]. In this paper we wish to report further investigations which we have carried out on this class of clusters in order to examine the factors that may be responsible for the unusually long bonds.

2. Results and discussion

2.1. Reactivity studies

The reaction of **1** with $AsPh_3$ afforded two new clusters, as shown in Scheme 1.

Both clusters have been completely characterised, including by single crystal X-ray diffraction studies; the ORTEP plots for **2** and **3** are given in Figs. 1 and 2, respectively. As in the case of the PPh_3 analogue **2a** (labeled as **4** in earlier report) [2a], cluster **2** is characterised by a very long Os–Os bond (~3.2 Å) bridged by an *o*-phenylene ligand. The arsine ligand is in an equatorial position on

* Corresponding author.
E-mail address: chmlwk@nus.edu.sg (W.K. Leong).

0022-328X/$ - see front matter © 2005 Elsevier B.V. All rights reserved.
doi:10.1016/j.jorganchem.2005.09.005

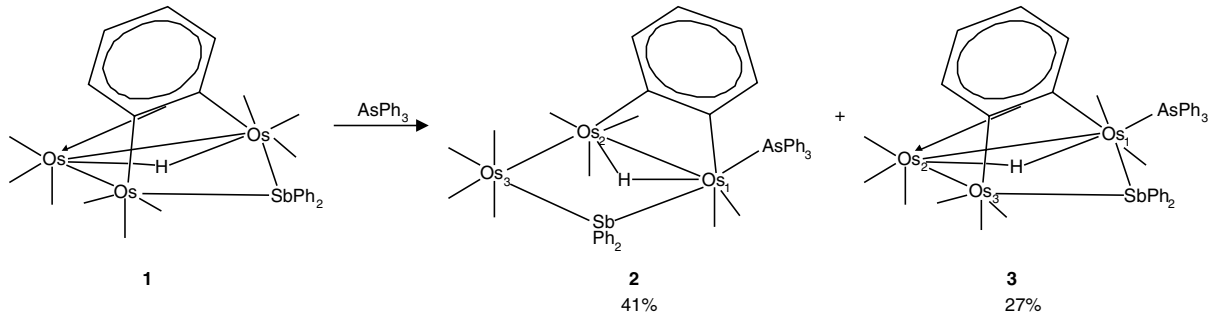

Scheme 1.

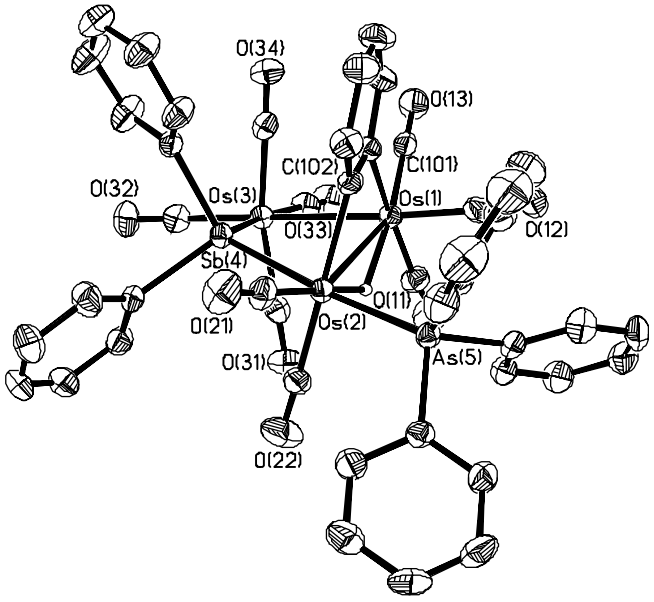

Fig. 1. ORTEP diagram and selected bond parameters of **2**. Thermal ellipsoids are drawn at 50% probability level. Organic hydrogens are omitted for clarity.

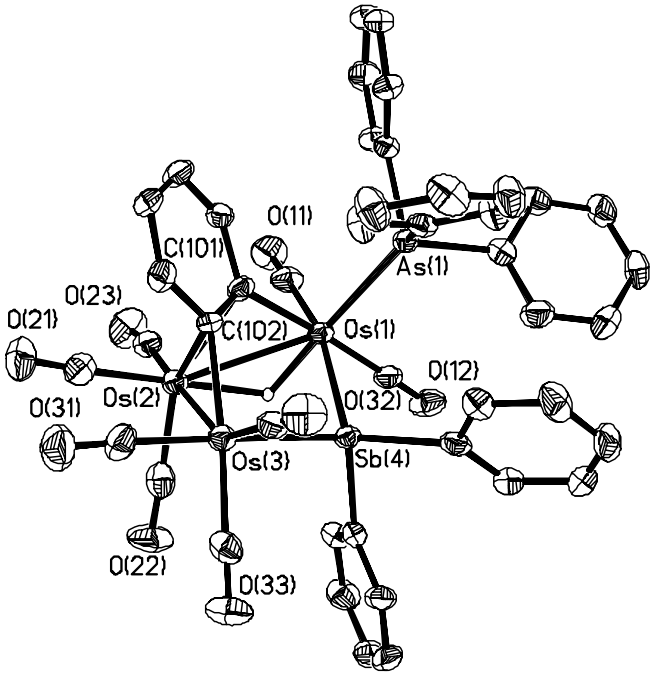

Fig. 2. ORTEP diagram and selected bond parameters of **3**. Thermal ellipsoids are drawn at 50% probability level. Organic hydrogens are omitted for clarity.

Os(1) (1,eq isomer; refer to Scheme 1 for Os atom labeling). Cluster **3** is the decarbonylated product of **2**, but it is a new and different positional isomer from the corresponding PPh_3 and PMe_2Ph analogues (labeled as **3a** and **3c**, respectively, in earlier report). In **3**, the arsine ligand is at an equatorial position on Os(1) (1,eq isomer) while in the phosphine analogues the phosphine ligand is at Os(2), in a pseudo-axial position (2,ax isomers).

The reaction of **1** with ^{t}BuNC afforded the adduct $Os_3(\mu\text{-}H)(SbPh_2)(\mu_2,\eta^2\text{-}C_6H_4)(CO)_9(CN^tBu)$, **4**, quantitatively. The structure of **4** has been confirmed by a single crystal X-ray crystallographic study and is shown in Fig. 3. Interestingly, **4** is structurally analogous to the initial adduct in the phosphine reactions (labelled clusters **2** in the earlier report) [2a]; the isonitrile ligand is in an equatorial position on Os(2) (2,eq isomer). On standing over a few days, or on heating, it was found that **4** isomerised to afford **5**. Monitoring the reaction by ^{1}H NMR spectroscopy showed that there were at least three other products ($\delta_{hydride} = -17.28$, -20.27 and -20.36 ppm) present in trace amounts, which we have not pursued further. The structure of **5** has also been confirmed by a single crystal X-ray diffraction study and the ORTEP plot is shown in Fig. 4. Unlike **4**, cluster **5** has the isonitrile in an axial position on Os(3) (3,ax isomer), on opposite side of the Os_3Sb plane from the *o*-phenylene. On the other hand, UV photolysis of **4** led to decarbonylation to afford $Os_3(\mu\text{-}H)(SbPh_2)(\mu_2,\eta^2\text{-}C_6H_4)(CO)_8(CN^tBu)$, **6**; some $Os_3(CO)_{12}$ was also observed to be formed. The ORTEP plot of **6** is shown in Fig. 5. Unlike the phosphine or arsine analogues, which are 2,ax and 1,eq isomers, respectively, the isonitrile ligand in **6** occupies an equatorial position on Os(2) (2,eq isomer).

The reactions involving ^{t}BuNC are summarised in Scheme 2. It is not clear how the isomerisation of **4** to **5** occurs, but it may involve migration of the isonitrile, possibly in tandem with carbonyl migration. Such an isonitrile migration, if non-dissociative, will imply involvement of a bridging isonitrile; compounds with isonitriles in such bonding modes are known [5]. The difference in behaviour

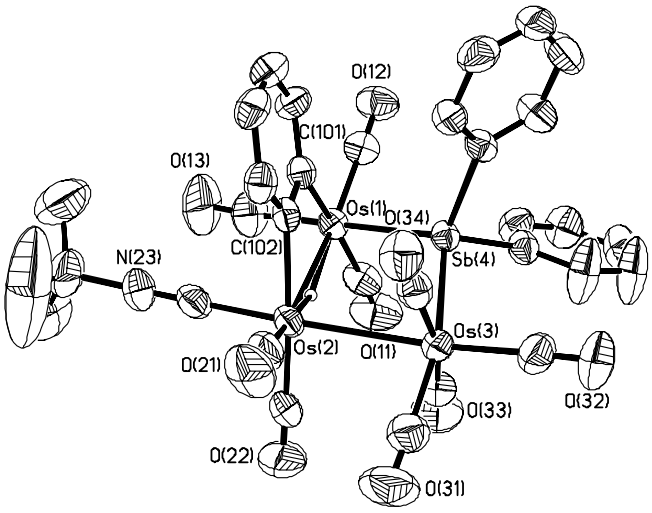

Fig. 3. ORTEP diagram and selected bond parameters of **4**. Thermal ellipsoids are drawn at 50% probability level. Organic hydrogens are omitted for clarity.

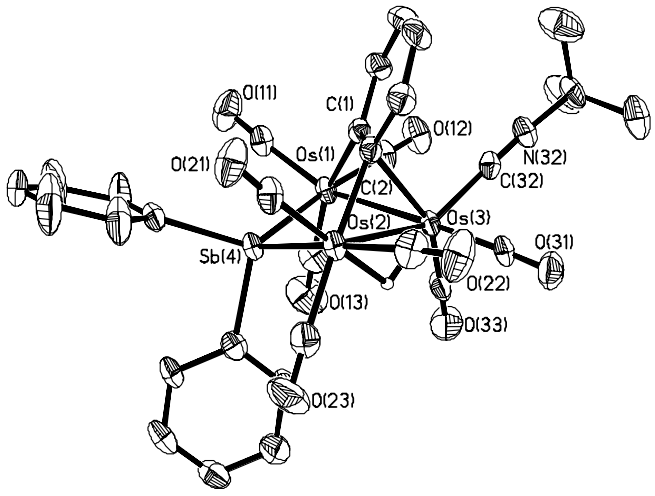

Fig. 5. ORTEP diagram and selected bond parameters of **6**. Thermal ellipsoids are drawn at 50% probability level. Organic hydrogens are omitted for clarity.

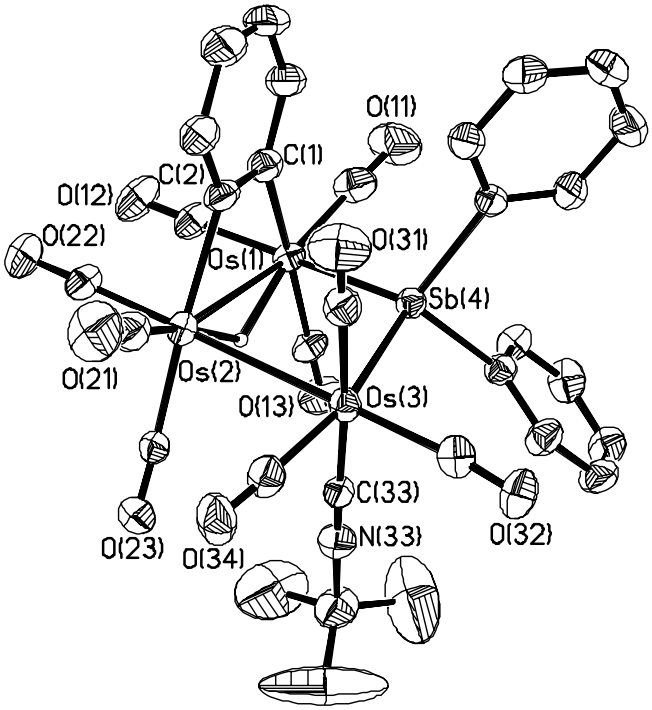

Fig. 4. ORTEP diagram and selected bond parameters of **5**. Thermal ellipsoids are drawn at 50% probability level. Organic hydrogens are omitted for clarity.

of **4** with the phosphine analogues is also interesting. In the latter case, we have earlier reported that the initial product is the 1,eq isomer, and this isomerises to the 2,eq isomer (and other pathways) [2a]. On the other hand, the observations here show that the initial adduct for isonitrile is the 2,eq isomer but the thermodynamically more stable isomer is the 3,ax. In one sense, that the axial isomer is preferred for isonitrile is anticipated [2g]. However, it is not obvious why the isonitrile should migrate to Os(3). That the isonitrile is *trans* to a metal–metal bond in **6** as opposed to a carbonyl in **5** cannot be the whole explanation since the isonitrile is similarly disposed in **4**.

2.2. Crystallographic studies

A common atomic numbering scheme and selected bond parameters for the adducts, including the previously reported phosphine analogues, are summarised in Table 1. A similar tabulation for the substitution derivatives of **1** is given in Table 2.

All the clusters **2**, **4** and **5** possess the characteristic long Os–Os bond that is bridged by the *o*-phenylene ligand. However, it is significant that the values for the isonitrile adducts are substantially lower than the 3.2 Å observed for the phosphine analogues; for **2**, although the value is also lower, the difference from that of **2a** is only $\sim 4\sigma$. On the other hand, the values for **4**, in which the isonitrile is *cis* to the Os_1–Os_2 bond, and **5**, in which the isonitrile is on Os_3, are quite comparable. These suggest that the elongation of the Os_1–Os_2 bond is partly due to the bridging *o*-phenylene and hydride, and also partly due to steric repulsion between the equatorial phosphine or arsine ligand with the carbonyl on the adjacent osmium; there is little electronic influence of the ligand. It is also interesting to observe that the Os_2–Os_3 bond in these clusters are also fairly long, all being ~3.0 Å; electronic effects from the ligand can be discerned here as the longest are to be found in **4a** and **4b** where the phosphines are *trans* to this bond.

This *trans* influence also manifests itself in the asymmetry of the Os–Sb bonds; the largest difference in the Os_1–Sb and Os_3–Sb bond lengths occur for **2** and **2a** (difference of 0.0527 and 0.0342 Å, respectively), compared to the smaller differences for the others (ranging from 0.0166 to 0.0043 Å). However, in this case, the Os–Sb bond *trans* to the ligand L is shorter than the other. This can be rationalised in terms of the dominance of π-bonding; the

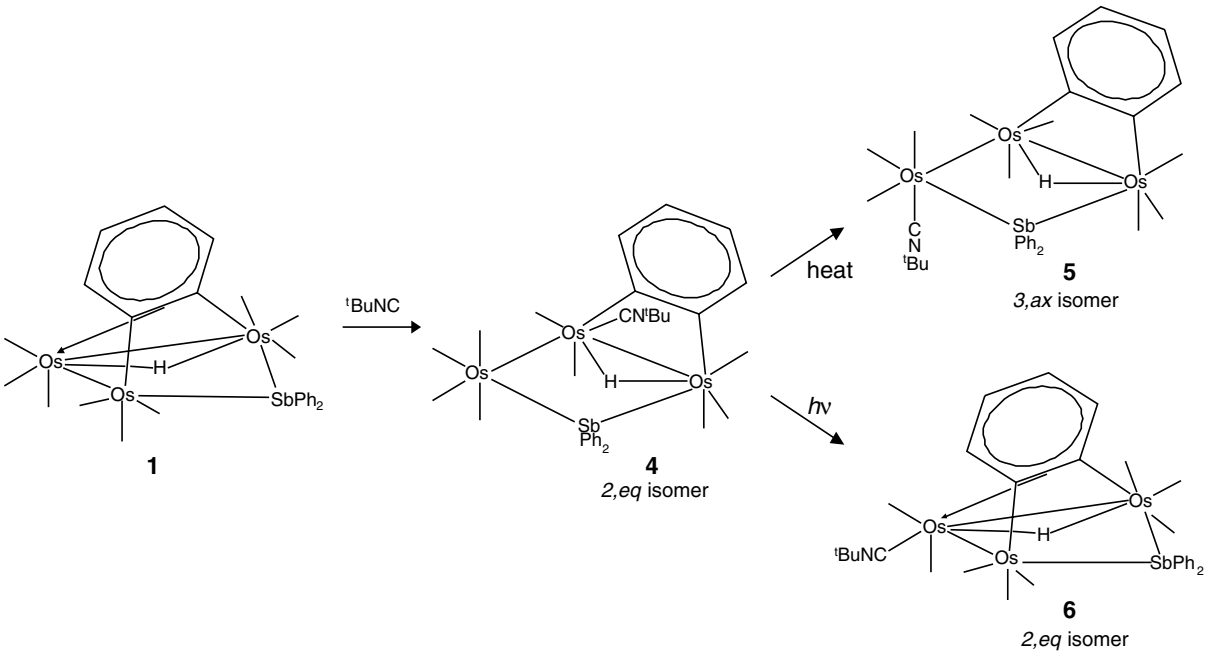

Scheme 2.

Table 1
Common atomic numbering scheme and selected bond parameters for the adducts **2**, **4** and **5**

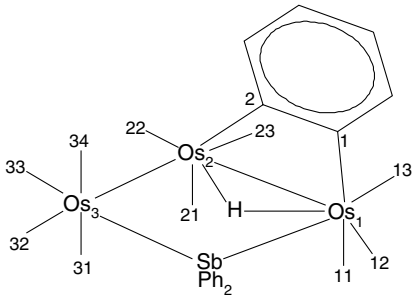

	2	**2a**[a]	**4**	**4a**[a]	**4b**[a]	**5**
Ligand (L)	$AsPh_3$	PPh_3	$CNBu^t$	PPh_3	$P(p\text{-tolyl})_3$	$CNBu^t$
Position of substitution	13	13	23	23	23	31
Bond lengths (Å)						
Os_1–Os_2	3.1991(3)	3.2025(8)	3.1823(3)	3.2332(12)	3.2308(3)	3.1806(3)
Os_2–Os_3	3.0014(3)	2.9999(8)	2.9999(3)	3.0298(13)	3.0454(4)	2.9746(3)
Os_1–Sb	2.6172(4)	2.6431(9)	2.6729(4)	2.6554(15)	2.6706(5)	2.6651(4)
Os_3–Sb	2.6699(4)	2.6773(11)	2.6886(4)	2.6717(11)	2.6663(5)	2.6817(4)
Os-L	2.4774(5)	2.382(3)	1.968(7)	2.365(2)	2.3593(17)	2.050(6)
Os_1–C_1	2.155(5)	2.160(13)	2.157(5)	2.123(10)	2.133(7)	2.156(6)
Os_1–C_2	2.168(5)	2.167(14)	2.141(6)	2.159(9)	2.145(6)	2.163(6)
C_1–C_2	1.407(8)	1.383(18)	1.412(8)	1.437(12)	1.408(9)	1.386(9)
Bond angles (°)						
Os_2–Os_1–Sb	75.511(9)	76.16(3)	77.290(10)	77.18(3)	78.400(12)	78.233(10)
Os_1–Os_2–Os_3	88.498(7)	88.75(2)	89.619(8)	88.88(3)	88.406(9)	89.257(8)
Os_2–Os_3–Sb	78.328(10)	79.33(3)	80.367(10)	80.68(4)	81.917(12)	81.791(11)
Os_1–Sb–Os_3	109.917(13)	109.31(4)	108.776(14)	110.90(5)	110.228(7)	108.034(14)

[a] From [2a].

order of π-acceptor ability is CO > EPh_3 > $SbPh_2$, and so consequently the Os_3–Sb interaction is weaker than that of Os_1–Sb as they are *trans* to a carbonyl [CO(33)] and an EPh_3, respectively. This is further corroborated by the observation that in the other clusters where there is no such a difference in the ligands *trans* to the Os–Sb bonds, the

Table 2
Common atomic numbering scheme and selected bond parameters for the derivatives **3** and **6**

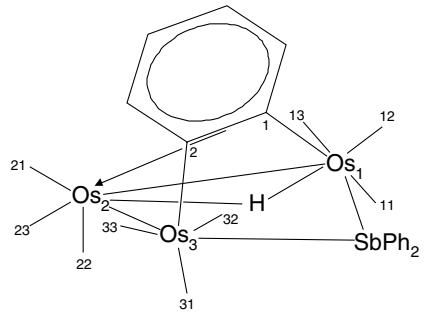

	3	**3a**[b]	**3b**[b]	**6**
Ligand (L)	$AsPh_3$	PPh_3	PMe_2Ph	$CNBu^t$
Position of substitution	31	22	22	23
Bond lengths (Å)				
Os_1–Os_2	2.9829(4)	2.9626(4)	3.0014(4)	2.9537(4)
Os_2–Os_3	2.8729(3)	2.9065(4)	2.8871(3)	2.8618(4)
Os_1–Sb	2.6485(4)	2.6565(6)	2.6574(5)	2.6568(6)
Os_3–Sb	2.6462(5)	2.6496(6)	2.6403(5)	2.6483(6)
Os–L	2.4846(7)	2.3566(19)	2.3194(17)	1.974(8)
Os_1–C_1	2.188(7)	2.176(8)	2.187(7)	2.186(8)
Os_3–C_2	2.160(6)	2.165(7)	2.168(6)	2.158(7)
Os_2–C_1	2.289(6)	2.342(7)	2.339(6)	2.338(7)
Os_2–C_2	2.371(6)	2.333(8)	2.350(6)	2.410(7)
C_1–C_2	1.448(10)	1.448(10)	1.451(9)	1.464(11)
Bond angles (°)				
Os_2–Os_1–Sb	78.861(13)	84.337(14)	82.426(12)	82.455(14)
Os_1–Os_2–Os_3	87.875(10)	87.502(11)	87.576(9)	88.108(11)
Os_2–Os_3–Sb	80.933(12)	85.580(14)	84.961(12)	84.390(15)
Os_1–Sb–Os_3	100.273(14)	99.806(18)	100.586(16)	99.342(17)

[b] From [2a].

bond lengths are generally closer to that for Os_3–Sb in **2** and **2a**. A similar effect may also be discerned when we compare the lengths of the Os–C(isonitrile) bond in **4** and **5**; that in the former is significantly shorter than that in the latter because of the bond being *trans* to a metal–metal bond and a carbonyl, respectively. Finally, we also noted that the longest sum of Os–C and C–O lengths are invariably associated with CO(11) and CO(21) [6], which are *trans* to the *o*-phenylene, and CO(31) and CO(34), which are *trans* to each other.

For the clusters **3** and **6**, the expectedly long metal–metal bond is that bridged by the hydride. There is close mirror symmetry through the molecule, especially for **3a** and **3b**. Thus little asymmetry between the Os–Sb bonds are expected, and indeed observed, the differences being below 0.0171 Å (for **3b**). Much of the asymmetry observed may probably be accounted for by the lengthening effects of the hydride bridge, an example being the asymmetry in the bond parameters associated with the μ_3,η^2–C_6H_4 unit. As has already been observed earlier [2a], the C_1–C_2 bond lengths in these clusters are all significantly longer than those in the adducts in Table 1, indicative of a greater loss of aromaticity in the μ_3,η^2 bonding mode.

3. Concluding remarks

We have shown that the reaction of **1** with arsine or isonitrile results in similar adduct formation as with phosphines, and these adducts are also possessed with a very long osmium–osmium bond. It is likely that this unusually long metal–metal bond may be attributed partly to the bridging *o*-phenylene and hydride, and in the case of the phosphines and arsine, partly to steric bulk of the ligand. It may therefore be expected that an even bulkier ligand may lead to even longer Os–Os bonds, although in all likelihood such a compound will also exhibit an increased propensity towards isomerisation or other subsequent reaction pathways.

4. Experimental

All reactions and manipulations were carried out under a nitrogen atmosphere by using standard Schlenk techniques. All solvents used in reactions were of AR grade, and were distilled from the appropriate drying agents prior to use. Separation of the cluster reaction products were generally by column chromatography on silica gel or by thin-layer chromatography (TLC), using plates coated with silica gel 60 F254 of 0.5 mm thickness. Photochemical reactions were performed with a Hanovia 450W UV lamp, with a nominal λ_{max} of 254 nm. Infrared spectra were recorded on a Bio-Rad FTS 165 FTIR spectrometer in a NaCl cell of 0.1 mm pathlength. NMR spectra were recorded on a Bruker ACF-300FT-NMR spectrometer in $CDCl_3$. Microanalyses were carried out by the microanalytical laboratory at the National University of Singapore. The cluster $Os_3(\mu\text{-}H)(\mu\text{-}SbPh_2)(\mu_3,\eta^2\text{-}C_6H_4)(CO)_9$, **1**, was prepared according to the previously published method [2e].

4.1. Reaction of *1* with $AsPh_3$

One equivalent of $AsPh_3$ (14.5 mg, 0.047 mmol) was added to a solution of **1** (55.8 mg, 0.047 mmol) in hexane (10 mL) in a schlenk tube under a flowing stream of N_2. The mixture was stirred at room temperature until the IR spectrum of the solution showed that **1** has been consumed (~7 d). Removal of the solvent followed by chromatographic separation on silica gel using dichloromethane/hexane (1/9, v/v) as eluant gave, in order of elution, faint yellow crystalline $Os_3(\mu\text{-}H)(SbPh_2)(\mu_2,\eta^2\text{-}C_6H_4)(CO)_9(AsPh_3)$ (**2**) (yield = 28.6 mg, 41.1%) and orange crystalline $Os_3(\mu\text{-}H)(SbPh_2)(\mu_3,\eta^2\text{-}C_6H_4)(CO)_8(AsPh_3)$ (**3**) (yield = 18.2 mg, 26.6%).

Analytical data for **2**. IR (hexane): ν_{CO} 2098m, 2056s, 2031m, 2022vs, 2009w, 1981w, 1956w cm^{-1}. ^1H NMR: δ_H 7.7–7.2 (m, 29H, aromatic), −18.71 (s, 1H, OsHOs). Calc. for $C_{45}H_{30}AsO_9Os_3Sb$: C, 36.47; H, 2.04. Found: C, 36.33; H, 1.93.

Analytical data for **3**. IR (hexane): ν_{CO} 2081m, 2035s, 2011s (br), 1960w (br), 1942m (br) cm^{-1}. ^1H NMR: δ_H 7.7–7.2 (m, 29H, aromatic), −17.58 (s, 1H, OsHOs). Calc.

Table 3
Crystal and refinement data for compounds **2**–**6**

Compound	**2**	**3**	**4**	**5**	**6**
Empirical formula	$C_{45}H_{30}AsO_9Os_3Sb \cdot 2CH_2Cl_2$	$C_{44}H_{30}AsO_8Os_3Sb$	$C_{32}H_{24}NO_9Os_3Sb$	$C_{32}H_{24}NO_9Os_3Sb$	$C_{31}H_{24}NO_8Os_3Sb \cdot 1/2C_6H_5CH_3$
Formula weight	1651.81	1453.95	1258.87	1258.87	1276.93
Temperature (K)	293(2)	173(2)	293(2)	223(2)	223(2)
Crystal system	Triclinic	Triclinic	Monoclinic	Monoclinic	Monoclinic
Space group	$P\bar{1}$	$P\bar{1}$	$P2_1/c$	$P2_1/n$	$C2/c$
a (Å)	12.9134(2)	11.5965(2)	16.3447(3)	12.63660(10)	34.0303(3)
b (Å)	13.2737(2)	11.6760(2)	13.21670(10)	13.41360(10)	9.62750(10)
c (Å)	15.9108(2)	16.6841(3)	17.0828(3)	21.3013(3)	22.91280(10)
α (°)	96.6790(10)	87.1610(10)	90	90	90
β (°)	106.6490(10)	78.9400(10)	95.6030(10)	99.01	103.6300(10)
γ (°)	103.6300(10)	68.9070(10).	90	90	90
Volume (Å^3)	2489.35(6)	2068.08(6)	3672.65(10)	3566.09(6)	7295.43(10)
Z	2	2	4	4	8
Density (calculated) (Mg/m^3)	2.204	2.335	2.277	2.345	2.325
Absorption coefficient (mm^{-1})	9.095	10.679	11.122	11.454	11.198
F(000)	1536	1340	2296	2296	4680
Crystal size (mm^3)	$0.38 \times 0.16 \times 0.10$	$0.32 \times 0.22 \times 0.16$	$0.41 \times 0.30 \times 0.24$	$0.38 \times 0.36 \times 0.22$	$0.22 \times 0.18 \times 0.15$
Θ range for data collection	2.28–29.35	1.87–29.34	2.25–29.26	2.02–29.29	2.20–29.39
Reflections collected	19257	15381	23691	23500	47715
Independent reflections [R_{int}]	11817 [0.0285]	9004 [0.0361]	9119 [0.0261]	8749 [0.0346]	8973 [0.0484]
Max. and min. transmission	0.297 and 0.163	0.264 and 0.120	0.180 and 0.111	0.127 and 0.060	0.316 and 0.149
Data/restraints/parameters	11817/0/590	9004/0/518	9119/0/419	8749/0/419	8973/2/416
Goodness-of-fit on F^2	1.060	1.034	1.158	1.123	1.065
Final R indices [$I > 2\sigma(I)$]	$R_1 = 0.0320$, $wR_2 = 0.0731$	$R_1 = 0.0361$, $wR_2 = 0.0868$	$R_1 = 0.0309$, $wR_2 = 0.0626$	$R_1 = 0.0325$, $wR_2 = 0.0711$	$R_1 = 0.0421$, $wR_2 = 0.0899$
R indices (all data)	$R_1 = 0.0416$, $wR_2 = 0.0785$	$R_1 = 0.0474$, $wR_2 = 0.0916$	$R_1 = 0.0440$, $wR_2 = 0.0691$	$R_1 = 0.0428$, $wR_2 = 0.0756$	$R_1 = 0.0605$, $wR_2 = 0.0996$
Largest diff. peak and hole (e Å^{-3})	1.292 and −1.359	2.358 and −2.501	0.605 and −1.231	1.130 and −1.872	2.875 and −2.929

for $C_{44}H_{30}AsO_8Os_3 \cdot CH_2Cl_2$: C, 35.12; H, 2.104. Found: C, 35.25; H, 1.88.

Presence of dichloromethane in the crystalline sample used for elemental analysis was confirmed by ^{1}H NMR spectroscopy.

4.2. Reaction of *1* with ^{t}BuNC

To a solution of **1** (35 mg, 0.030 mmol) in hexane (15 mL) was added excess ^{t}BuNC (2 drops). The mixture was stirred for 30 min until the IR spectrum of the solution showed that the starting material has been consumed. The solution was filtered through celite, concentrated, and then cooled to give pale yellow crystals of $Os_3(\mu\text{-H})(SbPh_2)(\mu_2,\eta^2\text{-}C_6H_4)(CO)_9(CN^tBu)$ (**4**). Yield = 28 mg, 74.7%. IR (CH_2Cl_2): ν_{CN} 2171m,br; ν_{CO} 2092m, 2077vs, 2011vs, 2002m, 1953m cm^{-1}. ^{1}H NMR: δ_H 7.7–6.2 (m, 14H, aromatic), 1.20 (s, 9H, ^{t}Bu), −19.47 (s, 1H, OsHOs). Calc. for $C_{32}H_{24}NO_9Os_3Sb$: C, 30.53; H, 1.92; N, 1.11. Found: C, 30.51; H, 2.00; N, 1.28.

4.3. Thermolysis of *4*

A hexane solution (15 ml) of **4** (21 mg, 0.017 mmol) was brought to reflux. The reaction was monitored by IR spectroscopy until all the starting material has been consumed (~6 h). The colour of the solution changed from pale yellow to bright yellow. The solvent was removed in vacuo and the residue recrystallised from CH_2Cl_2/hexane to give yellow crystals of $Os_3(\mu\text{-H})(SbPh_2)(\mu_2,\eta^2\text{-}C_6H_4)(CO)_9(CN^tBu)$ (**5**). Yield = 14 mg (67%). IR (CH_2Cl_2): ν_{CN} 2188w,br; ν_{CO} 2084m, 2067vs, 2043s, 2011s, 1993m,br, 1967m,br cm^{-1}. ^{1}H NMR: δ_H 7.9–6.0 (m, 14H, aromatic), 1.19 (s, 9H, ^{t}Bu), −20.75 (s, 1H, OsHOs). FAB-MS: 1258.9 (M^+). Calc. for $C_{32}H_{24}NO_9Os_3Sb$: C, 30.53; H, 1.92; N, 1.11. Found: C, 30.15; H, 1.97; N, 0.85.

4.4. Photolysis of *4*

A hexane solution (15 ml) of **4** (28 mg, 0.022 mmol) was placed in a quartz Carius tube, degassed by three freeze–pump–thaw cycles, and then irradiated under a UV lamp. The reaction was monitored by IR spectroscopy until all the starting material has been consumed. The solvent was removed in vacuo and the residue recrystallised from toluene/hexane to give orange crystals of $Os_3(\mu\text{-H})(SbPh_2)(\mu_2,\eta^2\text{-}C_6H_4)(CO)_8(CN^tBu)$ (**6**). Yield = 15 mg (55%). IR (hexane): ν_{CN} 2172w,br; ν_{CO} 2081m, 2043vs, 2010vs, 1996sh, 1973m, 1963m, 1953m cm^{-1}. ^{1}H NMR: δ_H 7.5–7.1 (m, 14H, aromatic), 1.32 (s, 9H, ^{t}Bu), −17.28 (s, 1H, OsHOs). FAB-MS: 1230.9 (M^+).

4.5. Crystal structure determinations

Crystals were grown from dichloromethane/hexane solutions and mounted on quartz fibres. X-ray data were collected on a Bruker AXS APEX system, using Mo Kα radiation, with the SMART suite of programs [7]. Data were processed and corrected for Lorentz and polarisation effects with SAINT [8], and for absorption effects with SADABS [9]. Structural solution and refinement were carried out with the SHELXTL suite of programs [10]. Crystal and refinement data are summarised in Table 3.

The structures were solved by direct or Patterson methods to locate the heavy atoms, followed by difference maps for the light, non-hydrogen atoms. Organic hydrogen atoms were placed in calculated positions and refined with a riding model. Metal hydrides were located in the difference maps and allowed to refine fully, except for **6** for which a fixed isotropic thermal parameter was assigned. All non-hydrogen atoms were generally given anisotropic displacement parameters in the final model (except for the solvent molecule in **6**).

There was a disordered toluene solvent molecule in **6**. The disorder is about a centre of inversion. Appropriate restraints were placed on the molecule, and the atoms were refined with isotropic thermal parameters.

5. Supplementary material

Crystallographic data (excluding structure factors) for the structures in this paper have been deposited with the Cambridge Crystallographic Data Centre as supplementary publication numbers CCDC 281862–281866. Copies of the data can be obtained, free of charge, on application to CCDC, 12 Union Road, Cambridge CB2 1EZ, UK, (fax: +44 1223 336033 or e-mail:deposit@ccdc.cam.ac.uk).

Acknowledgements

This work was supported by the National University of Singapore (Research Grant No. R143-000-190-112). G.C. and M.D. thank the University for Research Scholarships.

References

[1] K.H. Whitmire, Adv. Organomet. Chem. 42 (1998) 1.
[2] (a) G. Chen, M. Deng, C.K. Lee, W.K. Leong, Organometallics 21 (2002) 1227;
(b) M. Deng, W.K. Leong, Organometallics 21 (2002) 1221;
(c) M. Deng, W.K. Leong, J. Chem. Soc., Dalton Trans. (2002) 1020;
(d) W.K. Leong, G. Chen, Organometallics 20 (2001) 5771;
(e) W.K. Leong, G. Chen, Organometallics 20 (2001) 2280;
(f) W.K. Leong, G. Chen, J. Chem. Soc., Dalton Trans. (2000) 4442;
(g) G. Chen, W.K. Leong, J. Organomet. Chem. 574 (1999) 276;
(h) G. Chen, W.K. Leong, J. Chem. Soc., Dalton Trans. (1998) 2489.
[3] For examples of osmium–arsenic cluster chemistry, see (a) C.T. Tay, W.K. Leong, J. Organometal. Chem. 625 (2001) 231;
(b) K. Guldner, B.F.G. Johnson, J. Lewis, A.D. Massey, S. Bott, J. Organomet. Chem. 408 (1991) C13;
(c) K. Guldner, B.F.G. Johnson, J. Lewis, J. Organomet. Chem. 355 (1988) 419;

(d) K. Guldner, B.F.G. Johnson, J. Lewis, S.M. Owen, P.R. Raithby, J. Organomet. Chem. 341 (1988) C45;
(e) A.J. Deeming, R.E. Kimber, M. Underhill, J. Chem. Soc., Dalton Trans. (1973) 2589.
[4] A. Deeming, J. Adv. Organomet. Chem. 26 (1985) 6.
[5] For examples, see (a) M. Knorr, C. Strohmann, Organometallics 18 (1999) 248;
(b) H. Adams, N.A. Bailey, C. Bannister, M.A. Faers, P. Fedorko, V.A. Osborn, M.J. Winter, J. Chem. Soc., Dalton Trans. (1987) 341;
(c) H. Brunner, H. Buchner, J. Wachter, I. Bernal, W.H. Ries, J. Organomet. Chem. 244 (1983) 247.
[6] W.K. Leong, F.W.B. Einstein, R.K. Pomeroy, J. Cluster Sci. 7 (1996) 121.
[7] SMART version 5.628, Bruker AXS Inc., Madison, WI, USA, 2001.
[8] SAINT+ version 6.22a, Bruker AXS Inc., Madison, WI, USA, 2001.
[9] G.M. Sheldrick, SADABS, 1996.
[10] SHELXTL version 5.03, Siemens Energy & Automation Inc., Madison, WI, USA.